Dalton Transactions

Accepted Manuscript

ROYAL SOCIETY OF CHEMISTRY

www.rsc.org/dalton

Synthesis and photoelectric properties of new Dawson-type polyoxometalate-based dimeric and oligomeric Pt(II)-acetylide inorganic-organic hybrids

Li Liu,*[a] Lei Hu,[a] Qian Liu,[b] Zu-Liang Du,[c] Fa-Bao Li,*[a] Guang-Hua Li,[d] Xun-Jin Zhu,[b] Wai-Yeung Wong,*[b] Lei Wang,[e] and Hua Li[f]

[a] *Hubei Collaborative Innovation Center for Advanced Organic Chemical Materials, Ministry of Education Key Laboratory for the Synthesis and Application of Organic Functional Molecules, School of Chemistry and Chemical Engineering, Hubei University, Wuhan 430062, P. R. China*

E-mail: liulihubei@gmail.com; Fax: +86-2788663043; Tel: +86-2788662747

[b] *Institute of Molecular Functional Materials and Department of Chemistry and Partner State Key Laboratory of Environmental and Biological Analysis, Hong Kong Baptist University, Waterloo Road, Hong Kong, P. R. China*

[c] *Key Laboratory of Special Functional Materials, Henan University, Kaifeng 475001, P. R. China*

E-mail: rwywong@hkbu.edu.hk; Fax: +852-34117348; Tel:+852-34117074

[d] *State Key Laboratory of Inorganic Synthesis and Preparative Chemistry, College of Chemistry, Jilin University, Changchun 130012, P. R. China*

[e] *Wuhan National Laboratory for Optoelectronics, Huazhong University of Science and Technology, Wuhan, 430074, P. R. China.*

[f] *College of Life and Environmental Sciences & Beijing Engineering Research Center of Food Environment and Public Health, Minzu University of China, Beijing 100081, P. R. China*

A new synthesis route for preparing Dawson-type polyoxometalate (POM) based inorganic-organic hybrid material is presented. Two new heteropolytungstate-based dimeric and oligomeric Pt(II) acetylide inorganic-organic hybrid compounds (2PtOD and PPtOD) were prepared by Hagihara's dehydrohalogenating coupling of a terminal diacetylene POM hybrid containing diphosphoryl functionality and an appropriate platinum(II) halide precursor. This method provides a rigid covalent linkage between the POM and the organometallic Pt(II) acetylide moiety. The redox potential of the polyanion can be tuned by grafting the organic and organometallic groups on it. The photoelectric properties of hybrid LB films derived from these inorganic-organic composites were studied.

Introduction

Polyoxometalates (POM) constitute a large class of inorganic compounds with remarkable chemical, structural and electronic versatility that have found applications in a diversity of areas ranging from catalysis to medicine and materials science.[1] A salient feature of POMs is their ability to reversibly accept several electrons and therefore to act as electron reservoirs with good redox tuning capability.[2] As a result, POMs are attractive candidates for the development of photochemical devices aiming at photocumulative electron transfer. However, their electrostatic[3] or covalent attachment to a light-harvesting antenna is desirable, since POMs themselves are indeed photoactive but only in the UV part of the solar spectrum.[4] Although POMs have been widely used for the preparation of hybrid materials and functional molecular devices,[5] it is still a great challenge to realize organic-functionalized POMs.

Since the pioneering work of Peng and Wei on the organic derivatives of Lindqvist POMs,[6] Proust and Izzet have developed the phase transfer conditions applicable to the functionalization of mono-,[7] di-,[8] or tri-vacant POMs.[9] Very few examples have been reported in which the POM is covalently connected to a photoactive antenna. Recently, Odobel, Izzet, Nomiya and Villanneau reported a family of Dawson-type POMs di-functionalized with organo-silyl or organo-phosphoryl moieties.[10] Some synthetic tools adopting classical reactions such as Sonogashira and Huisgen couplings have been realized from organic synthesis to POM derivatization.

Carbon-rich organometallic functional materials with rigid, π-conjugated chains

have also aroused considerable attention and may lead to various advanced applications[11] such as lasers, photocells and organic light-emitting diodes. They possess particularly promising electronic and structural properties, including nonlinear optical effects,[12] luminescence and photoconductivity,[13] electronic communication in molecular wires,[14] and liquid crystallinity.[15] Harvesting of organic triplet emissions harnessed through the strong heavy-atom effects of group 10–12 metals was also extensively probed in molecular and polymeric Pt-acetylide systems.[16]

As continuation of our research efforts[16,17] in this field and the application of POM-based hybrids in the development of photochemical devices, we started our work in grafting the rigid, π-conjugated group 10 platinum(II) diyne and polyyne chains as photoactive antenna to the redox-active Dawson heterpolytungstate via classical CuI-catalyzed Hagihara's dehydrohalogenating coupling reaction. To our knowledge, there are no literature reports on covalent post-functionalization of POMs with Pt(II)-acetylide groups by such dehydrohalogenating coupling reaction to form Pt–C bond. Such a methodology allows the connection of the POM to the organometallic entity via a rigid linker. Furthermore, this simple and efficient synthetic route can be potentially extended to a large number of transition metal chromophores. We describe here the synthesis of two novel POM-based inorganic-organic hybrids by the covalent bonding of Pt(II)-acetylide units in dimeric and oligomeric structures (Fig. 1).

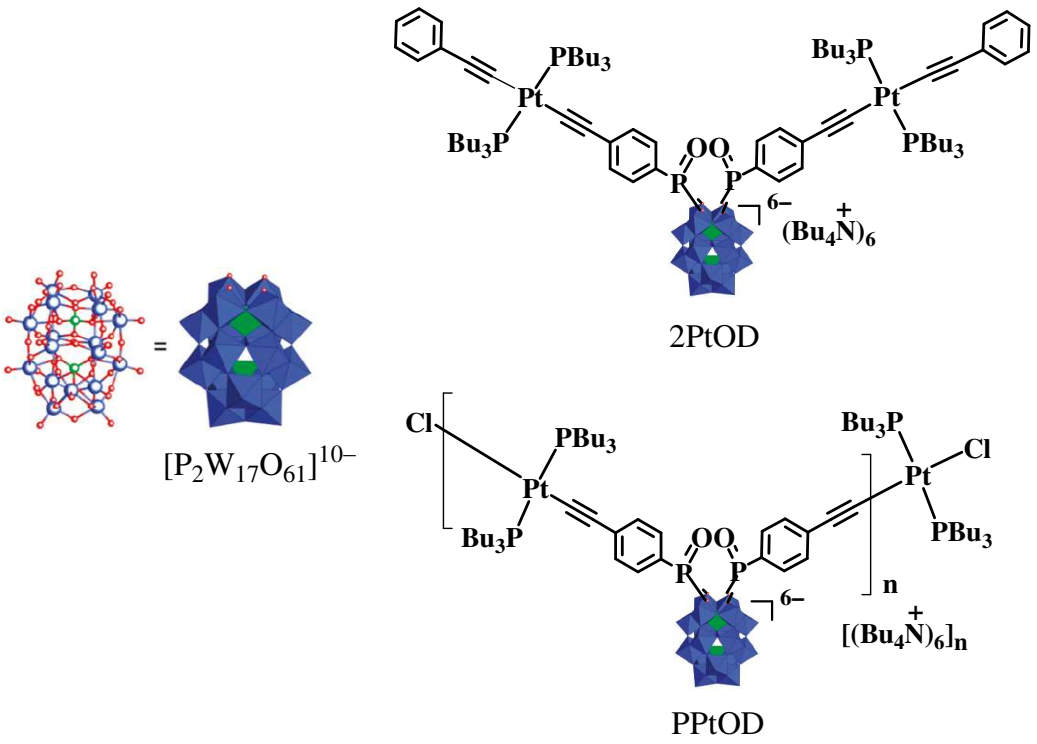

Fig. 1 Structures of 2PtOD and PPtOD

Results and discussion

Synthesis and chemical characterization

Lacunary POMs differ from the complete POMs by their charge, shape and electronic properties which result in different nucleophilicity. Odobel and co-workers[10a] described the synthesis of the POM-based hybrid $(NBu_4)_6[P_2W_{17}O_{61}(P(O)C_6H_4C{\equiv}CH)_2]$ (OD) as a tetrabutylammonium (TBA) salt. We modified the reaction condition that aqueous HCl was added to the reaction system consisting of 4-ethynylphenyl phosphonic acid (H_2O_3P-C_6H_4-C≡CH, abbreviated as O) and $K_{10}[P_2W_{17}O_{61}]$ (D), in which the apparent pH of the solution was fixed at 2, and OD was obtained with a slightly higher yield of 80% than that from the literature method. In addition, an

excess of O is required to stimulate the completion of reaction and improve the purity of the resulting compound.

One novelty of this work lies in its synthetic strategy to graft Pt(II)-acetylide units to POM. All the POM-based metal alkynyl complexes and oligomers were obtained in good yields by the general reaction routes described in Scheme 1. The POM-based dinuclear Pt(II) complex (2PtOD) can be considered as the molecular model and building block of POM-based long chain organometallic oligomer (PPtOD). PPtOD and 2PtOD were synthesized by CuI-catalyzed dehydrohalogenating coupling of *trans*-[$PtCl_2(PBu_3)_2$] or *trans*-[$PtCl(PBu_3)_2(C{\equiv}CPh)$] (PtClPh) with OD under a weakly basic (Et_3N) condition at room temperature (r.t.) as depicted in Scheme 1.[17b] It should be noted that the amount of Et_3N added is no more than the equivalent amount of the HCl produced in order to keep the stability of POM. The feed mole ratios of the platinum(II) chloride precursors and the POM-based diethynyl ligand were 2:1 and 1:1 for the model complex and oligomer syntheses, respectively, and each product was carefully purified by selective precipitation. Silica and alumina gel chromatographic separation cannot be adopted for the purification of these POM-based hybrids since they would result in their adsorption or degradation.

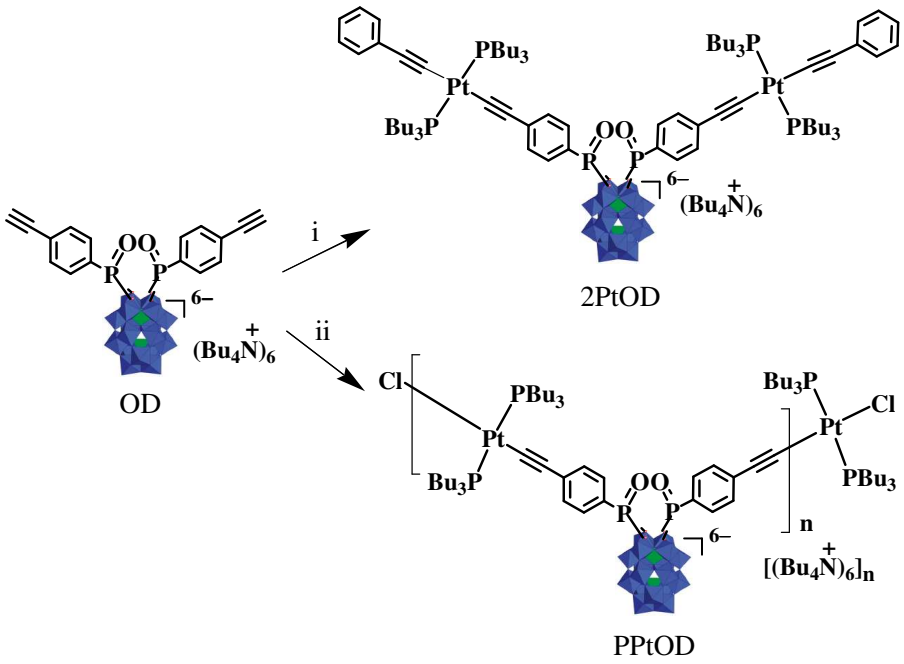

Scheme 1. Synthetic routes to the organo-diphosphoryl POM-based hybrids. (i) *trans*-[$PtCl(PBu_3)_2(C\equiv CPh)$], CuI, Et_3N, CH_3CN; (ii) *trans*-[$PtCl_2(PBu_3)_2$], CuI, Et_3N, CH_3CN.

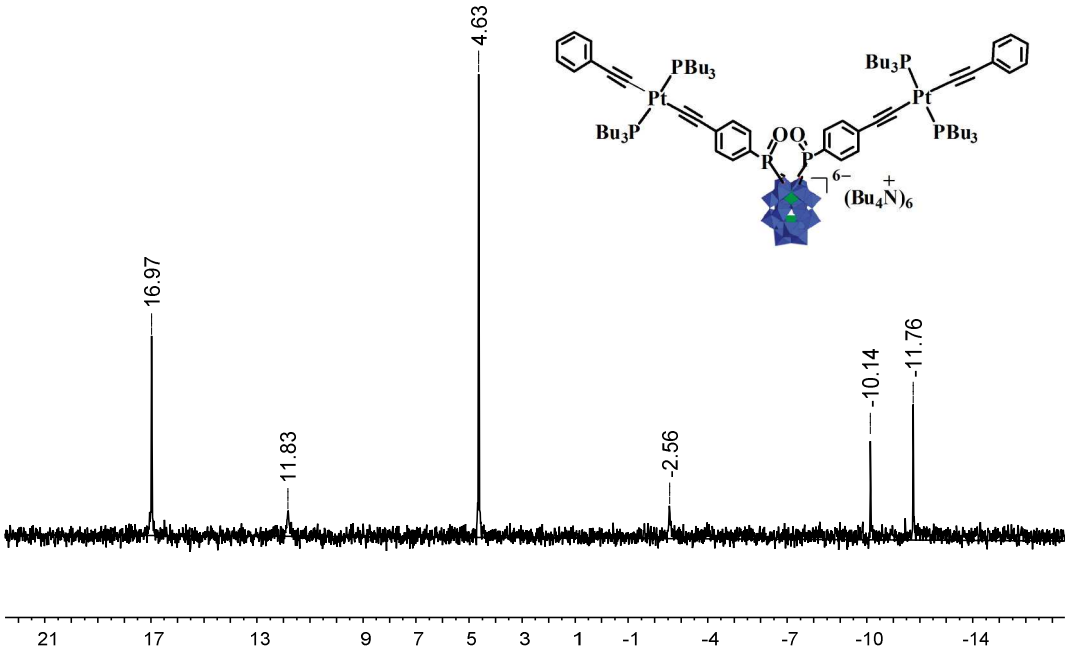

Fig. 2 ^{31}P NMR spectrum of 2PtOD in CD_3CN.

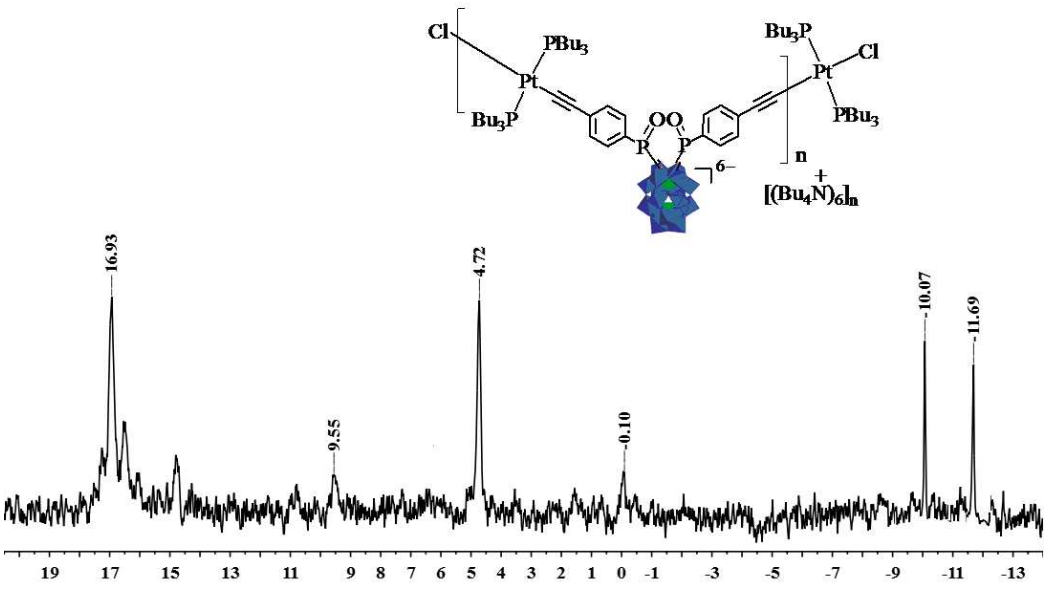

Fig. 3 ^{31}P NMR spectrum of PPtOD in CD_3CN.

All the new POM-based Pt(II) complex and oligomer are air-stable and can be stored without demanding any special precautions. They generally exhibit good solubility in acetonitrile, DMF and DMSO, but are insoluble in hydrocarbons, alcohols and ethers. While all attempts to grow single crystals of 2PtOD have met with little success so far, systematic characterization of these POM-based Pt(II) compounds was achieved by analytical and spectroscopic methods. The ^{1}H NMR spectra of 2PtOD and PPtOD (shown in Electronic Supplementary Information) gave peaks corresponding to protons in the counter cation Bu_4N^+ (3.10, 1.60, 1.35, and 0.96 ppm) and PBu_3 (2.07, 1.53, 1.40, 0.86 ppm) which appear at nearly identical chemical shifts in both spectra. The proton signals arising from the aromatic groups were observed clearly. The symmetrical nature of all complexes was evident from the NMR spectral pattern. The single ^{31}P-{^{1}H} NMR signal flanked by platinum satellites for

each of 2PtOD and PPtOD is consistent with a *trans* geometry of the square planar Pt(II) unit (Figs. 2 and 3) . The $^{1}J_{P\text{-}Pt}$ values in 2PtOD and PPtOD are typical for related *trans*-PtP_2 systems.[18] The peaks at 4.63 ppm for 2PtOD and 4.72 ppm for PPtOD are attributed to the PBu_3 group. The P=O signal is observed at nearly identical chemical shifts for both hybrids (16.97 for 2PtOD and 16.93 ppm for PPtOD). The signals at -10.14 and -11.76 ppm for 2PtOD as well as -10.07 and -11.69 ppm for PPtOD are due to the PW_8 and PW_9 group of Dawson type polyoxometalate $P_2W_{17}O_{61}$, respectively.

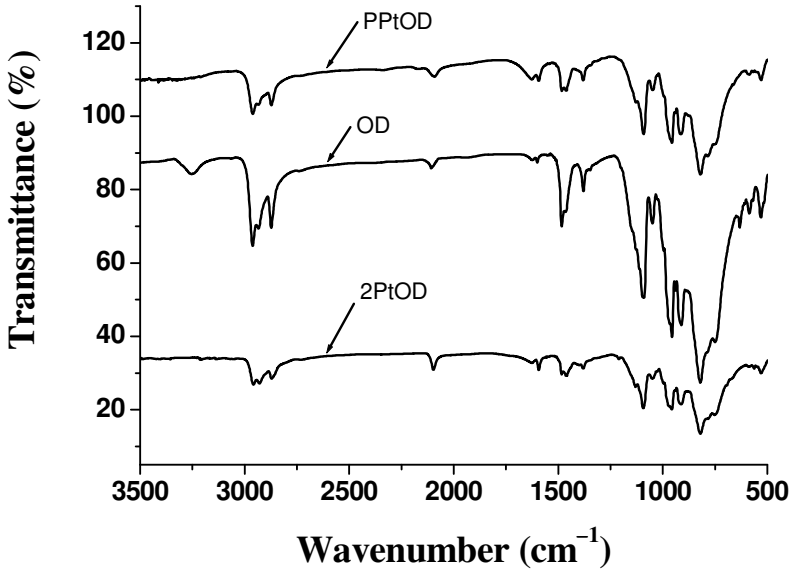

Fig. 4 IR spectra of OD, 2PtOD and PPtOD.

The IR spectra of compounds 2PtOD and PPtOD resemble that of the OD (Fig. 4). In the low wavenumber region (< 1100 cm^{-1}), OD, 2PtOD and PPtOD display a pattern characteristic of the Dawson structure: four strong bands of the P–O_a, W–O_d, W–O_b–W and W–O_c–W asymmetric stretching vibrations at ca. 1092, 956, 913 and

785 cm^{-1}, respectively.[10a] Weak IR ν(C≡C) absorption bands at ca. 2097 and 2091 cm^{-1} for 2PtOD and PPtOD, respectively, are similar to those observed for the di- and poly-nuclear Pt(II) diethynyl complex.[16] The IR spectra of 2PtOD and PPtOD show no characteristic ≡C–H stretching vibration band in the range of 3200–3300 cm^{-1}, thus confirming that the OD core is capped by metal groups via σ bonds.

We can locate an intense molecular ion peak (HM^{5-}) in the MALDI-TOF mass spectrum for 2PtOD. The molecular weight of the oligomer PPtOD was also measured by MALDI-TOF technique. The aggregated ions, charge state, and their *m/z* values including the calc. values are shown in the Experimental Section. The number of repeating unit n of PPtOD is calculated as 5, and the elemental analyses of 2PtOD and PPtOD confirm the composition of the hybrids. The lack of discernible ^1H resonance and IR absorption attributed to the C≡C-H end groups in the NMR and IR spectra suggests the presence of *trans*-$Pt(PBu_3)_2Cl$ as end groups for PPtOD.

Redox and photophysical properties

Cyclic voltammetry studies of D, OD, PPtOD and 2PtOD were carried out with $TBAPF_6$ as the supporting electrolyte and a saturated calomel electrode (SCE) as the reference (see Fig. 5). The values of reduction wave potential E_{pc} of D, OD, PPtOD and 2PtOD are listed in Table 1. Four cathodic peak potentials were seen at –0.91, –1.21, –1.64 and –1.85 V for D, which correspond to the reduction of POM.[19] Compared with the cathodic peak potentials of D, hybrid compound OD displayed the POM reduction at more anodic peak potentials of –0.24, –0.58, –1.16 and –1.45 V,

due to the electron-withdrawing effect of HC≡C-C_6H_4-P=O moiety on the POM. A similar anodic shift was reported for the hybrid POM disubstituted with phenyl-phosphoryl moiety.[20] PPtOD and 2PtOD displayed one POM-based reduction wave with the potential value of –1.51 and –1.54 V, respectively, which is likely due to the 3- or 4-electrons reduction process. A comparison of the redox potentials of D with PPtOD and 2PtOD indicates that the organometallic group exhibits an opposite effect as compared to that observed with the organic group. Thus, the redox potential of the polyanion can be tuned by grafting the organic and organometallic groups on it.

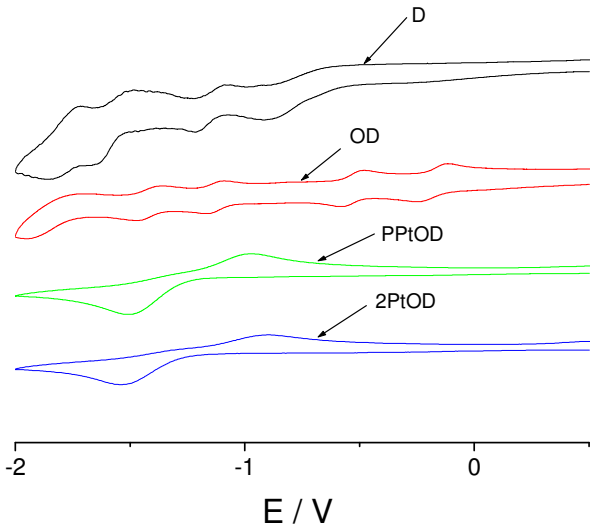

Fig. 5 Cyclic voltammogram of a 10^{-4} M solution of D, OD, PPtOD and 2PtOD in acetonitrile containing 0.1 M $TBAPF_6$: scan rate, 200 mV s^{-1}; working electrode, glassy carbon; reference electrode, SCE.

Table 1. The values of reduction wave potentials of D, OD, PPtOD and 2PtOD.

Compound	E_{pc1} (V)	E_{pc2} (V)	E_{pc3} (V)	E_{pc4} (V)

D	–0.91	–1.21	–1.64	–1.85
OD	–0.24	–0.58	–1.16	–1.45
PPtOD	–	–	–1.51	–
2PtOD	–	–	–1.54	–

The solution UV-Vis absorption spectra of O, D, OD, PtClPh, 2PtOD and PPtOD are shown in Fig. 6. The hybrids OD, 2PtOD and PPtOD displayed strong absorption bands in the near UV region. These bands are mainly associated with the organic π–π* transitions, possibly mixed with some admixture of metal orbitals. For D and the three hybrid compounds OD, 2PtOD and PPtOD, they all exhibited intense $O_d \rightarrow W$ charge-transfer transition peak at ca. 196–206 nm (where O_d represents the terminal oxygen in the POM).[21] Compared with the lowest-energy electronic transition at 236 nm in O, such transition for OD is bathochromically shifted by 22 nm. This indicates that there is an obvious electronic transition between the metal-oxygen cluster and the conjugated organic segment in the hybrid. Similar bathochromic shift can be seen in 2PtOD and PPtOD (see Table 2). Compared with the lowest-energy electronic transition at 307 nm in PtClPh, such transition for 2PtOD and PPtOD is bathochromically shifted by 33 and 38 nm, respectively. This indicates that the delocalization of organometallic conjugated π electrons has extended from the Pt ethynylphenyl unit to the $P_2W_{17}O_{61}$ skeleton. In other words, there is a strong electronic interaction between the metal–oxygen cluster and the conjugated organometallic segment(s) in the hybrid compounds.

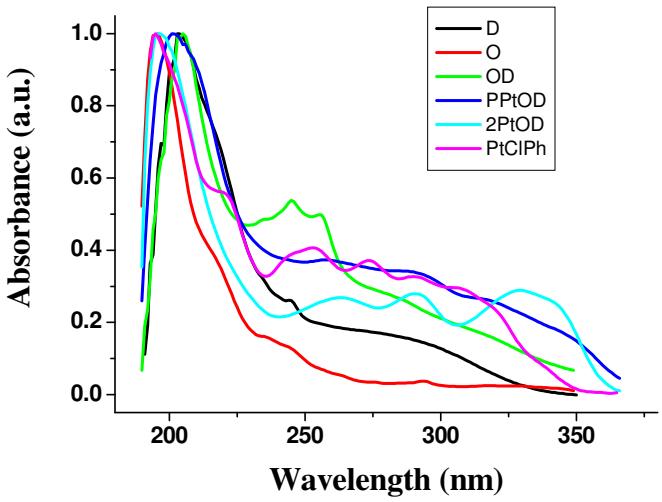

Fig. 6 UV-Vis spectra of 4-ethynylphenyl phosphonic acid (O), D, OD, 2PtOD, PPtOD and PtClPh in CH_3CN.

Table 2. Absorption data for the compounds

Compound	λ_{max} (nm)
D	203, 245
O	195, 236
OD	206, 245, 258
PtClPh	195, 220, 253, 273, 292, 307
2PtOD	196, 262, 291, 327, 340
PPtOD	201, 258, 290, 317, 345

The fluorescence spectra of 4-ethynylphenyl phosphonic acid (O), D, OD and PPtOD were measured in acetonitrile (Fig. 7). Compared with the luminescence of $K_{10}P_2W_{17}O_{61}$ (391 nm) and the free 4-ethynylphenyl phosphonic acid (394 nm), the hybrids OD and PPtOD are less fluorescent than the precursor O. Compared with OD and PtClPh, the luminescence of PPtOD is less fluorescent. Presumably, the nonemissive LMCT excited state quenches more of the π–π* transition states of

PPtOD than that of OD. The PL spectra of 2PtOD were also measured at room temperature and 77 K, in which we observe intense $^1(\pi\pi^*)$ fluorescence band at 364 nm and weak $(\pi\pi^*)^3$ phosphorescence band at 468 nm. Compared with the phosphorescence peak at room temperature, the intensity at 77 K decreases slightly, whereby the $P_2W_{17}O_{61}$ causes quenching of the Pt phenylethynyl phosphorescence to a certain extent, presumably by accepting the excited electrons.

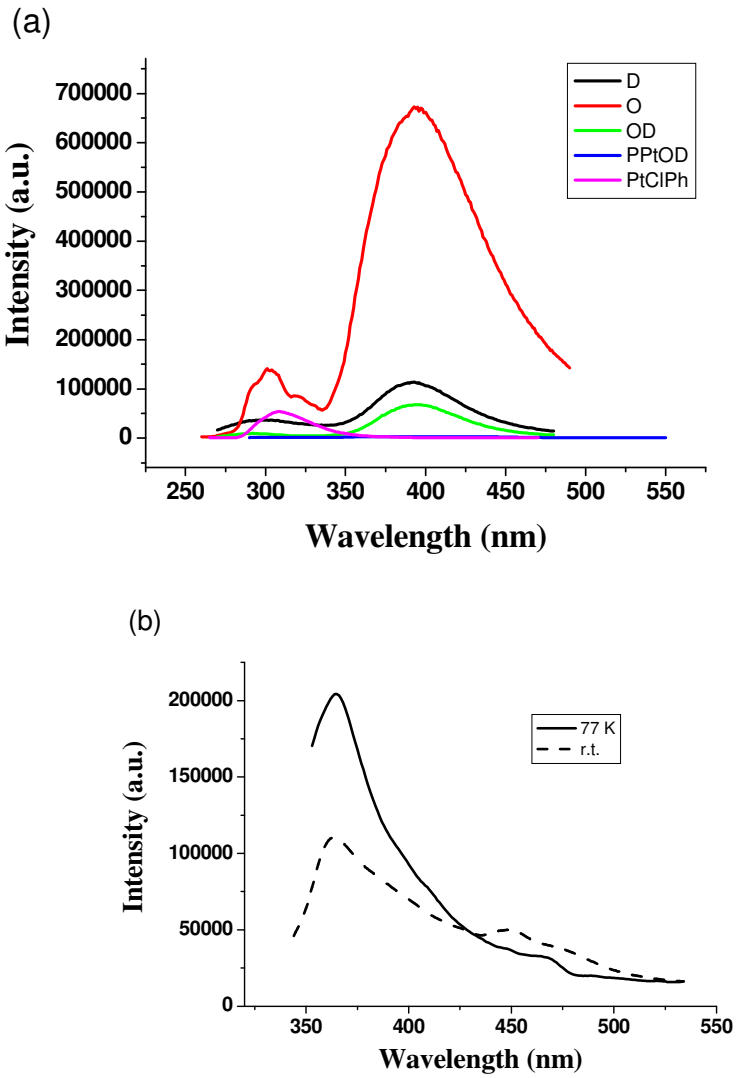

Fig. 7 Photoluminescence spectra of (a) 4-ethynylphenyl phosphonic acid (O), D, OD and PPtOD in CH_3CN. (b) 2PtOD at r.t. and 77 K in CH_3CN.

Langmuir-Blodgett film characterization and photoelectric effect

Langmuir-Blodgett (LB) film of PPtOD can be organized as monolayers using the LB technique and arachidic acid (AA) plays only a structural role in ensuring a good-quality LB film for PPtOD. Surface characterization of the LB films by atomic force microscopy (AFM) has also been performed. The image and structure of the hybrid monolayer film deposited on mica was measured (Fig. 8). The AFM image of PPtOD/AA shows that the hybrid LB film consists of disperse particles with different domain sizes of 74–87 nm. The average surface roughness (*R*a) is 0.49 nm and the largest roughness (*R*z) is 4.62 nm.

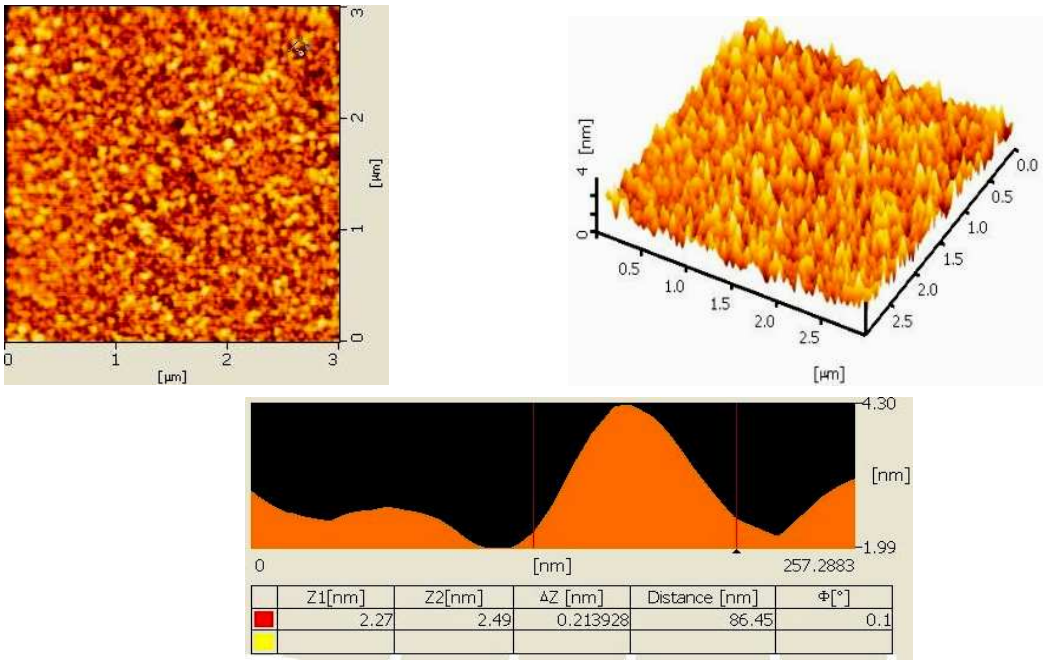

Fig. 8 AFM image of the PPtOD monolayer LB film.

The photovoltaic effect of the 13-layer PPtOD hybrid LB film deposited on the ITO wafer was also studied following UV irradiation using the surface photovoltage spectroscopy (SPS) technique. The results are shown in Fig. 9. The PPtOD hybrid LB

film displayed obvious photovoltage effect in the UV-Vis region. The photovoltage response can be as high as 2 μV at 466 nm. It is known that Pt-phenylethynyl complex which contains π-conjugated electrons can serve as an electron donor, whereas the $P_2W_{17}O_{61}$ core is a photosensitive substance and can act as an electron acceptor. Presumably, it is the electron transfer between the electron donor and acceptor that is believed to be the main cause for the observed photoelectric effect of the hybrid LB film. When the LB film was excited by light, the photovoltaic effect becomes a key factor.

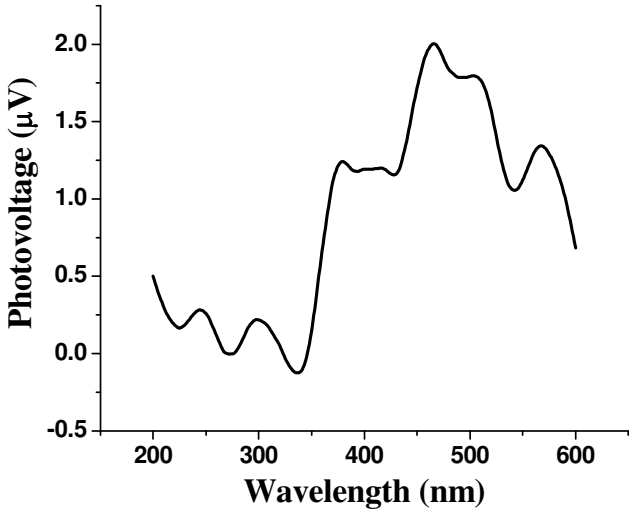

Fig. 9 Surface photovoltage response of the hybrid LB film (13 layers) of PPtOD.

The electric conductivity behavior of PPtOD 3-layer LB film on ITO wafer was examined using scanning tunneling microscopy. When the voltage was monitored at –1.3 to 2.6 V, the tunneling current obtained is 100 nA to –100 nA. A representative *I*–*V* plot is shown in Fig. 10 for such a device. It should be noted that Pt-phenylethynyl complex is a very poor conductor in the intrinsic state but our hybrid LB composite in the device can be semiconducting. The Pt-phenylethynyl complex is

a π-electron rich compound (electron donor), and $P_2W_{17}O_{61}$ is easily reducible (electron acceptor). We anticipated that when the two components are fabricated in an inorganic/organic hybrid, good electrical conductivity might demonstrate the origin of electron transfer from Pt-phenylethynyl to $P_2W_{17}O_{61}$. Another possible reason is the good electron mobility of POM, which is capable of offering some electrical conductivity.[22]

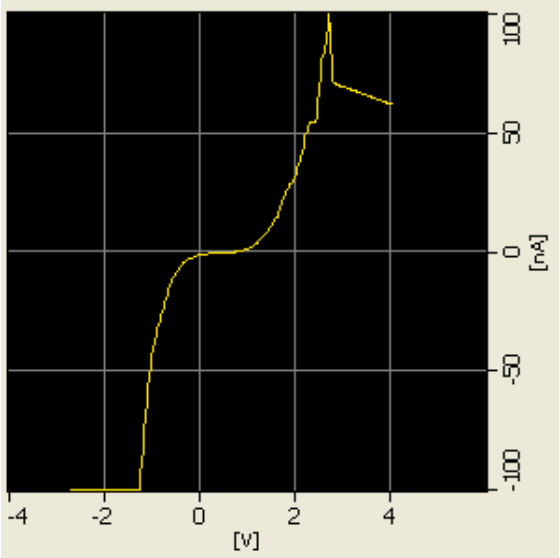

Fig. 10 The *I–V* curve of a 3-layer film on ITO wafer for PPtOD.

Concluding remarks

In summary, we describe here a new methodology for the covalent attachment of an organometallic linker to a polyoxometalate di-functionalized with organo-phosphoryl unit. In fact, the realization of organic functionalization of POM has become a current challenge of inorganic chemistry. These as-synthesized hybrid compounds and their LB and photoelectric properties were well characterized by sufficient experimental data, which could support the conclusion of the work. As expected, the grafting of the

organo and organometallic phosphoryl units on the POM has evident effect on the redox properties of the polyanion. This synthetic route can be extended to a wide range of accessible POM hybrids that could be used for many other applications (e.g. photovoltaic devices and molecular memories). Such dimeric and oligomeric Pt(II) acetylide-POM hybrids can be used to build a new inorganic/organic hybrid system for photoelectric application.

Experimental section

Materials

Analytical grade solvents were purified by distillation over appropriate drying agent under an inert nitrogen atmosphere prior to use. All reagents and chemicals, unless otherwise stated, were purchased from commercial sources and used without further purification. The compounds $K_{10}[\alpha_2\text{-}P_2W_{17}O_{61}]\cdot 20H_2O$ (D),[23] *trans*-$[PtCl_2(PBu_3)_2]$,[24] *trans*-$PtCl(PBu_3)_2(C{\equiv}CPh)$,[25] and 4-ethynylphenyl phosphonic acid[26] were synthesized according to the published procedures.

Instrumentation

Infrared spectra were recorded from KBr pellets on a Nicolet iS10 FTIR spectrometer. ^1H and ^{31}P NMR spectra were recorded on a VARIAN 600 MHz NMR spectrometer, using deuterated solvents as the lock and reference. Chemical shifts were reported in ppm relative to $SiMe_4$ for ^1H and 85% H_3PO_4 for ^{31}P nucleus. Cyclic voltammetry at a carbon electrode was carried out using the ZAHNER IM6 system. A standard

three-electrode cell was used, which consisted of the working vitrous carbon electrode, an auxiliary platinum electrode, and an aqueous saturated calomel electrode (SCE) equipped with a double junction. The scan rate was 200 mV s^{-1}. Each studied product was dissolved in distilled acetonitrile at a concentration of 10^{-4} M using $TBAPF_6$ as the electrolyte (10^{-1} M). The high performance triple quadrupole time-of-flight mass spectra were obtained using API QSTAR Pulsar/LC/MS/MS system mass spectrometer operated in the negative ion mode. C, H, N, Cl analyses were determined by using a Vario Micro Cube elemental analyzer. Pt and W were determined by using an inductively coupled plasma (ICP) atomic absorption spectrometer (Optimal 8000, USA). UV-Vis spectra were measured on a UNICAM Heλios α spectrometer. PL spectra were recorded on a SPEX F212 fluorescence spectrometer. Surface photovoltage spectroscopy (SPS) was measured on a D-300 surface photovoltage instrument. Photoluminescence spectra were recorded on a SPEX F212 fluorescence spectrometer. Atomic force microscopy (AFM) image and scanning tunneling microscopy (STM) of the LB films were measured on a SPA-400 atomic force microscope.

Monolayer and LB film fabrication

PPtOD can be organized as a monolayer using the LB technique in which arachidic acid (AA) was used in ensuring a good-quality LB film for PPtOD. Monolayer formation and deposition were carried out on a French LB 105 slot under room temperature condition at 20 ± 1 °C under a continuous dry nitrogen flow. The surface

pressure was measured by the Wilhelmy plate method. Triple-distilled water at pH = 6 with a resistivity higher than 1.8×10^5 Ωm and surface tension of 70 mN m^{-1} was used as the subphase. The spreading solution of PPtOD and AA (2:1, 1.0×10^{-4} mmol L^{-1}) in the mixture of acetonitrile and chloroform (v/v, 1:2) was spread onto the pure water subphase using a microsyringe. Compression began at a compression rate of 0.3 cm^2 min^{-1} after the solvent was evaporated for 45 min and the isotherms were recorded. All the experiments for monolayer deposition were performed under a surface pressure of 5 mN m^{-1}. In the case where a stable Langmuir monolayer of PPtOD/AA film was formed on the subphase, the monolayer was subsequently deposited onto the substrate [indium tin oxide (ITO) substrate for current–voltage (*I*–*V*) and SPS] by the vertical dipping method at a rate of 3 mm min^{-1}, resulting in a fairly good deposition of a typical Y-mode film. The number of layers of LB film prepared here is equal to the number of dipping or lifting processes, on each of which a floating Langmuir monolayer was transferred onto the substrate with a good transfer ratio of ca. 1.

Synthesis of OD

To a solution of 4-ethynylphenyl phosphonic acid (0.6 g, 1.6 mmol) in CH_3CN (50 mL) stirred at room temperature was added solid $K_{10}[\alpha_2\text{-}P_2W_{17}O_{61}]\cdot 20H_2O$ (2 g, 0.4 mmol) and solid NBu_4Br (1.68 g, 5.2 mmol). After 15 min, 12.4 M HCl (0.13 mL) was added to the mixture to adjust the pH to 2. After refluxing the mixture for 2 h, the mixture was cooled to room temperature and the light yellow product was filtered,

washed vigorously with ethanol and water, and dried with diethyl ether to yield **OD** (2.08 g, 0.32 mmol, 80%) as a light yellow powder. ^{1}H-NMR (DMSO-d_6): δ = 7.94–7.98 (m, 4H, ArH), 7.55–7.57 (m, 4H, ArH), 4.36 (s, 2H, CH), 3.16 (t, J = 20.5 Hz, 48H, CH_2N), 1.55–1.59 (m, 48H, CH_2CH_2N), 1.32 (sextuplet, J = 20.5 Hz, 48H, CH_2CH_3), 0.93 (t, J = 20.5 Hz, 72H, CH_3). ^{31}P-NMR (CD_3CN): δ = 14.97 (m, P(O)), –10.14 (s, PW_8), –11.70 ppm (s, PW_9). IR (KBr, cm^{-1}): ν = 3254 (s), 3063 (s), 2106 (w), 1146 (w), 1110 (w), 1092 (vs), 1043 (s), 1030 (w), 975 (vs), 921 (vs), 905 (vs), 819 (vs), 809 (vs), 740 (vs).

Synthesis of 2PtOD

A mixture of *trans*-$PtCl(PBu_3)_2(PhC{\equiv}C)$ (20.1 mg, 0.0287 mmol) and OD (80.7 mg, 0.0136 mmol) was dissolved in CH_3CN (5 mL) and CuI (3 mg) and NEt_3 (0.1 mL) were subsequently added. After stirring at room temperature for 12 h, all the volatile compounds were removed under reduced pressure. The residue was redissolved in CH_3CN and filtered. Diethyl ether (30 mL) was added to the filtrate and a brown red precipitate appeared. The crude solid was recovered by centrifugation. For purification purpose, the compound was dissolved in CH_3CN, and diethyl ether was then added with a similar volume to initiate precipitation. After several times of purification, **2PtOD** (73.4 mg, 0.01 mmol, 74%) was obtained as a brown red solid. ^{1}H-NMR (CD_3CN): δ = 7.93 (d, J = 24.0 Hz, 4H, ArH), 7.32 (d, J = 11.3 Hz, 4H, ArH), 7.22 (q, J = 7.7 Hz, 8H, ArH), 7.13 (t, J = 6.7 Hz, 2H, ArH), 3.20–3.04 (m, 48H, $NCH_2CH_2CH_2CH_3$), 2.28–2.15 (m, 24H, $PCH_2CH_2CH_2CH_3$), 1.63 (d, J = 6.1 Hz,

72H, $NCH_2CH_2CH_2CH_3$ and $PCH_2CH_2CH_2CH_3$), 1.44–1.48 (m, 24H, $PCH_2CH_2CH_2CH_3$), 1.38–1.42 (m, 48H, $NCH_2CH_2CH_2CH_3$), 0.99 (t, J = 6.0 Hz, 72H, $NCH_2CH_2CH_2CH_3$), 0.92 (t, J = 6.0 Hz, 36H, $PCH_2CH_2CH_2CH_3$). ^{31}P-NMR (CD_3CN): δ = 16.97 (m, P(O)), 4.63 ($J_{Pt\text{-}P}$ = 2345 Hz, Bu_3P), –10.14 (s, PW_8), –11.76 (s, PW_9). IR (KBr, cm^{-1}): ν = 3070 (s), 2957 (s), 2928 (s), 2871 (s), 2730 (s), 2097 (w), 1625 (w), 1593 (s), 1485 (s), 1463 (s), 1399 (s), 1379 (s), 1211 (s), 1130 (w), 1093 (s), 1052 (w), 1049 (w), 1026 (w), 997 (w), 970 (s), 957 (s), 940 (w), 920 (s), 911 (w), 821 (s), 784 (s), 753 (s), 693 (w), 585 (w), 563 (w), 531 (w), 478 (w). MS (MALDI-TOF): *m*/*z* calcd for $C_{80}H_{126}O_{63}P_8Pt_2W_{17}$ 1172.1102, found 1172.0632 $[(HM)^{5-}]$. Anal calcd for $C_{176}H_{342}O_{63}P_8Pt_2W_{17}N_6$ (%): C, 28.90; H, 4.71; Pt, 5.33; W, 42.73. Found: C, 29.55; H, 4.87; Pt, 5.21; W, 42.80.

Synthesis of PPtOD

A mixture of *trans*-$PtCl_2(PBu_3)_2$ (11.3 mg, 0.0169 mmol) and OD (100.2 mg, 0.0169 mmol) was dissolved in CH_3CN (5 mL) and CuI (3 mg) and NEt_3 (0.1 mL) were subsequently added. After stirring at room temperature for 12 h, all the volatile compounds were removed under reduced pressure. The residue was redissolved in CH_3CN and filtered. Diethyl ether (30 mL) was added to the filtrate and a brown red solid was precipitated. The crude solid was recovered by centrifugation. For purification, the compound was dissolved in CH_3CN and diethyl ether was then added with a similar volume to initiate precipitation. After several times of purification, **PPtOD** (86.2 mg, 0.01 mmol, 78%) was isolated as a brown red solid. ^{1}H-NMR

(CD_3CN): δ = 7.94 (d, *J* = 24 Hz, 4H, ArH), 7.33 (d, *J* = 10.1 Hz, 4H, ArH), 3.15 (s, 48H, $NCH_2CH_2CH_2CH_3$), 2.18–2.15 (m, 12H, $PCH_2CH_2CH_2CH_3$), 1.65 (s, 60H, $PCH_2CH_2CH_2CH_3$ and $NCH_2CH_2CH_2CH_3$), 1.42 (s, 60H, $NCH_2CH_2CH_2CH_3$ and $PCH_2CH_2CH_2CH_3$), 1.00 (s, 72H, $PCH_2CH_2CH_2CH_3$), 0.96–0.91 (m, 18H, $NCH_2CH_2CH_2CH_3$). ^{31}P-NMR (CD_3CN): δ = 16.93 (m, P(O)), 4.72 (s, J_{Pt-P} = 3494 Hz, Bu_3P), –10.07 (s, PW_8), –11.69 (s, PW_9). IR (KBr, cm^{-1}) ν = 2962 (s), 2909 (s), 2870 (s), 2176 (w), 2092 (w), 1628 (s), 1460 (s), 1384 (w), 1128 (w), 1092 (s), 1049 (w), 1026 (w), 994 (w), 956 (s), 941 (w), 913 (s), 820 (s), 785 (s), 750 (s), 662 (w), 587 (w), 529 (w). Anal calcd for $C_{704}H_{1444}Cl_2N_{30}O_{315}P_{32}Pt_6W_{85}$ (%): C, 25.45; H, 4.38; Cl, 0.21; N, 1.26; Pt, 3.52; W, 47.03. Found: C, 25.59; H, 4.52; Cl, 0.20; N, 1.29; Pt, 3.37; W, 47.28.

Sample	Charge State	Ion *m/z*	Calcd value	Aggregate
PPtOD (n = 5)	28	945.6089	944.4476	$[TBA_2M]^{28-}$
	26	1007.6359	1007.8942	$[H_3TBAM]^{26-}$
	20	1408.0430	1407.0763	$[HTBA_9M]^{20-}$
	10	2864.7772	2863.4095	$[H_9TBA_{11}M]^{10-}$

Acknowledgements

This work was supported by the National Natural Science Foundation of China (Nos. 21071049 and 51373145), Natural Science Foundation of Hubei Province of China (2013CFA087), Hubei Province High-End Talent Training Program and Natural Science Fund for Creative Research Groups of Hubei Province of China. W.-Y. Wong acknowledges the financial support from the National Basic Research Program of

China (973 Program) (2013CB834702), Hong Kong Research Grants Council (HKBU203313 and HKUST2/CRF/10), Areas of Excellence Scheme, University Grants Committee of HKSAR, China (Project No. AoE/P-03/08) and Hong Kong Baptist University (FRG2/12-13/083). H. Li thanks the 111 Project and Beijing Engineering Research Center of Food Environment and Public Health from Minzu University of China (No. B08044 and No.10301-01404026) for financial support. The work was also supported by Partner State Key Laboratory of Environmental and Biological Analysis and Strategic Development Fund of HKBU.

References

(1) (a) Thematic Issue on Polyoxometalates, *Chem. Rev.*, 1998, **98**, 1–388. (b) T. Yamase and M. T. Pope, (Eds.), *Polyoxometalate Chemistry for Nano-composite Design*, Kluwer Academic/Plenum Publishers, New York, 2002. (c) M. T. Pope, *Heteropoly and Isopoly Oxometalates*, Berlin, Springer, 1983. (d) M. T. Pope and A. Müller (Eds.), *Polyoxometalate Chemistry: From Topology Via Self-Assembly to Applications*, Kluwer, Dordrecht, The Netherlands, 2001. (e) J. J. Borrás-Almenar, E. Coronado, A. Müller and M. T. Pope, (Eds.), *Polyoxometalate Molecular Science*, Kluwer, Dordrecht, The Netherlands, 2001.

(2) (a) J. Zhang, A. M. Bond, D. R. MacFarlane, S. A. Forsyth, J. M. Pringle, A. W. A. Mariotti, A. F. Glowinski and A. G. Wedd, *Inorg. Chem.*, 2005, **44**, 5123-5126. (b) N. Fay, E. Dempsey and T. McCormac, *J. Electroanal. Chem.*, 2005, **574**, 359–366. (c) M. Zynek, M. Serantoni, S. Beloshapkin, E. Dempsey

and T. McCormac, *Electroanalysis* (N. Y.), 2007, **19**, 681–689.

(3) (a) M. K. Seery, L. Guerin, R. J. Forster, E. Gicquel, V. Hultgren, A. M. Bond, A. G. Wedd and T. E. Keyes, *J. Phys. Chem. A*, 2004, **108**, 7399–7405. (b) N. Fay, V. M. Hultgren, A. G. Wedd, T. E. Keyes, R. J. Forster, D. Leane and A. M. Bond, *Dalton Trans.*, 2006, **35**, 4218–4227. (c) J. Zhu, I. I. Walsh, A. M. Bond, T. E. Keyes, and R. J. Foester, *Langmuir*, 2012, **28**, 13536–13541. (d) J. J. Walsh, J. Zhu, Q. Zeng, R. J. Forster and T. E. Keyes, *Dalton Trans.*, 2012, **41**, 9928–9937. (e) J. J. Walsh, D. L. Long, L. Cronin, A. M. Bond, R. J. Forster and T. E. Keyes, *Dalton Trans.*, 2011, **40**, 2038–2045.

(4) (a) E. Papaconstantinou, *Chem. Soc. Rev.*, 1989, **18**, 1–31. (b) A. Troupis, E. Gkika, T. Triantis, A. Hiskia and E. Papaconstantinou, *J. Photochem. Photobiol., A,* 2007, **188**, 272–278. (c) C. L. Hill, D. A. Bouchard, M. Kadkhodayan, M. M. Williamson, J. A. Schmidt and E. F. Hilinski, *J. Am. Chem. Soc.*, 1988, **110**, 5471–5479. (d) R. F. Renneke, M. Pasquali and C. L. Hill, *J. Am. Chem. Soc.*, 1990, **112**, 6585–6594. (e) D. C. Duncan, T. L. Netzel and C. L. Hill, *Inorg. Chem.*, 1995, **34**, 4640–4646. (f) T. Ruther, V. M. Hultgren, B. P. Timko, A. M. Bond, W. R. Jackson and A. G. Wedd, *J. Am. Chem. Soc.,* 2003, **125**, 10133–10143. (g) T. Yamase, X. O. Cao and S. Yazaki, *J. Mol. Catal. A: Chem.,* 2007, **262**, 119–126.

(5) (a) A. Proust, R. Thouvenot and P. Gouzerh, *Chem. Commun.*, 2008, 1837–1852. (b) A. Dolbecq, E. Dumas, C. R. Mayer and P. Mialane, *Chem. Rev.*, 2010, **110**, 6009–6048. (c) A. M. Douvas, E. Makarona, N. Glezos, P. Argitis, J. A.

Mielczarski and E. Mielczarski, *ACS Nano*, 2009, **2**, 733–742.

(6) B. B. Xu, Y. G. Wei, C. L. Barnes and Z. H. Peng, *Angew. Chem. Int. Ed.*, 2001, **40**, 2290–2292.

(7) D. Agustin, J. Dallery, C. Coelho, A.Proust and R. Thouvenot, *J. Organomet. Chem.*, 2007, **692**, 746–754.

(8) (a) C. R. Mayer, I. Fournier and R. Thouvenot, *Chem. Eur. J.*, 2000, **6**, 105–110. (b) C. R. Mayer, P. Herson and R. Thouvenot, *Inorg. Chem.*, 1999, **38**, 6152–6158.

(9) (a) A. Mazeaud, N. Ammari, F. Robert and R. Thouvenot, *Angew. Chem., Int. Ed. Engl.,* 1996, **35**, 1961–1964. (b) D. Agustin, C. Coelho, A. Mazeaud, P. Herson, A. Proust and R. Thouvenot, *Z. Anorg. Allg. Chem.*, 2004, **630**, 2049–2053. (c) C. R. Mayer and R. Thouvenot, *J. Chem. Soc., Dalton Trans.,* 1998, 7–13.

(10) (a) A. K. Harriman, J. Elliott, M. A. H. Alamiry, L. Le Pleux, M. Severac, Y. Pellegrin, E. Blart, C. Fosse, C. Cannizzo, C. R. Mayer and F. Odobel, *J. Phys. Chem. C*, 2009, **113**, 5834–5842. (b) F. Odobel, M. Severac, Y. Pellegrin, E. Blart, C. Fosse, C. Cannizzo, C. Mayer, R. K. J. Eliott and A. Harriman, *Chem. Eur. J.*, 2009, **15**, 3130–3138. (c) K. J. Elliott, A. Harriman, L. L. Pleux, Y. Pellegrin, E. Blart, C. R. Mayerc and F. Odobel, *Phys. Chem. Chem. Phys.*, 2009, **11**, 8767–8773. (d) B. Matt, S. Renaudineau, L. M. Chamoreau, C. Afonso, G. Izzet and A. Proust, *J. Org. Chem.* 2011, **76**, 3107–3112. (e) B. Matt, C. Coudret, C. Viala, D. Jouvenot, F. Loiseau, G. Izzet and A. Proust, *Inorg. Chem.*, 2011, **50**, 7761–7768. (f) K. Nomiya, Y. Togashi, Y. Kasahara, S. Aoki, H. Seki, M.

Noguchi and S. Yoshida, *Inorg. Chem.*, 2011, **50**, 9606–9619. (g) R. Villanneau, A. Marzouk, Y. Wang, A. Djamaa, G. Laugel, A. Proust and F. Launay, *Inorg. Chem.*, 2013, **52**, 2958–2965.

(11) (a) N. J. Long and C. K. Williams, *Angew. Chem., Int. Ed.*, 2003, **42**, 2586–2617. (b) L. Liu, W. H. Ai, M. J. Li, S. Z. Liu, C. M. Zhang, H. X. Yan, Z. L. Du and W.-Y. Wong, *Chem. Mater.*, 2007, **19**, 1704–1711.

(12) (a) M. I. Bruce, *Chem. Rev.*, 1998, **98**, 2797–2858. (b) S. Barlow and D. O'Hare, *Chem. Rev.*, 1997, **97**, 637–669. (c) I. R. Whittal, A. M. McDonagh and M. G. Humphrey, *Adv. Organomet. Chem.*, 1998, **42**, 291–362.

(13) (a) I. Manners, *Synthetic Metal-Containing Polymers*; Wiley: Weinheim, Germany, 2004. (b) W.-Y. Wong and C. L. Ho, *Coord. Chem. Rev.*, 2006, **250**, 2627–2690.

(14) F. Paul and C. Lapinte, *Coord. Chem. Rev.*, 1998, **178**, 431–509.

(15) D. W. Bruce and D. O'Hare, Eds.; *Inorganic Materials*; Wiley: Chichester, 1996.

(16) (a) W.-Y. Wong, L. Liu, S. Y. Poon, K. H. Choi, K. W. Cheah and J. X. Shi, *Macromolecules*, 2004, **37**, 4496–4504. (b) L. Liu, S. Y. Poon and W.-Y. Wong, *J. Organomet. Chem.* 2005, **690**, 5036–5048.

(17) (a) L. Liu, W.-Y. Wong, J.-X. Shi and K.-W. Cheah, *J. Polym. Sci. A: Polym. Chem.*, 2006, **44**, 5588–5607. (b) L. Liu, W.-Y. Wong, J.-X. Shi, K.-W Cheah, T.-H. Lee and L. M. Leung, *J. Organomet. Chem.*, 2006, **691**, 4028–4041. (c) L. Liu, C.-L. Ho, W.-Y. Wong, K.-Y. Cheung, M.-K. Fung and W.-T. Lam, *Adv. Funct. Mater.*, 2008, **18**, 2824–2833. (d) L. Liu, W. Y. Wong, S. Y. Poon, J. X.

Shi, K. W. Cheah and Z. Y. Lin, *Chem. Mater.*, 2006, **18**, 1369–1378.

(18) M. S. Khan, M. R. A. Al-Mandhary, M. K. Al-Suti, B. Ahrens, M. F. Mahon, L. Male, P. R. Raithby, C. E. Boothby and A. Köhler, *Dalton Trans.,* 2003, 74–84.

(19) (a) X. L. Wang and M. Zhao, *An Introduction to Electrochemistry of Polyoxometalates*, *China Environmental Science Press*, Beijing, 2006. (b) J. Ni, Z. Zhou, L. Liu, S. Z. Liu, F. B. Li and Z. L. Du, *Aust. J. Chem.,* 2014, http://dx.doi.org/10.1071/CH14028.

(20) M. Boujtita, J. Boixel, E. Blart, C.R. Mayer and F. Odobel, *Polyhedron*, 2008, **27**, 688–692.

(21) E. B. Wang, C. W. Hu and L. Xu, *An Introduction to Heteropolyacid*, *Chemical Engineering Press*, Beijing, 1998.

(22) L. C. Palilis, M. Vasilopoulou, A. M. Douvas, D. G. Georgiadou, S. Kennou, N. A. Stathopoulos, V. Constantoudis and P. Argitis, *Solar Energy Mater. Solar Cells*, 2013, **114**, 205–213.

(23) R. Contant, *Inorg. Synth.*, 1990, **27**, 104–111.

(24) J. Chatt and R. G. Hayter, *J. Chem. Soc. Dalton Trans.*, 1961, 896–904.

(25) J. Chatt, B. L. Shaw, *J. Chem. Soc.*, 1960, 4020–4032.

(26) H. Onouchi, K. Maeda and E. Yashima, *J. Am. Chem. Soc.* 2001, **123**, 7441–7442.

Graphical abstract

Synthesis and photoelectric properties of new Dawson-type polyoxometalate-based dimeric and oligomeric Pt(II)-acetylide inorganic-organic hybrids

Li Liu, Lei Hu, Qian Liu, Zu-Liang Du, Fa-Bao Li, Guang-Hua Li, Xun-Jin Zhu, Wai-Yeung Wong, Lei Wang, Hua Li

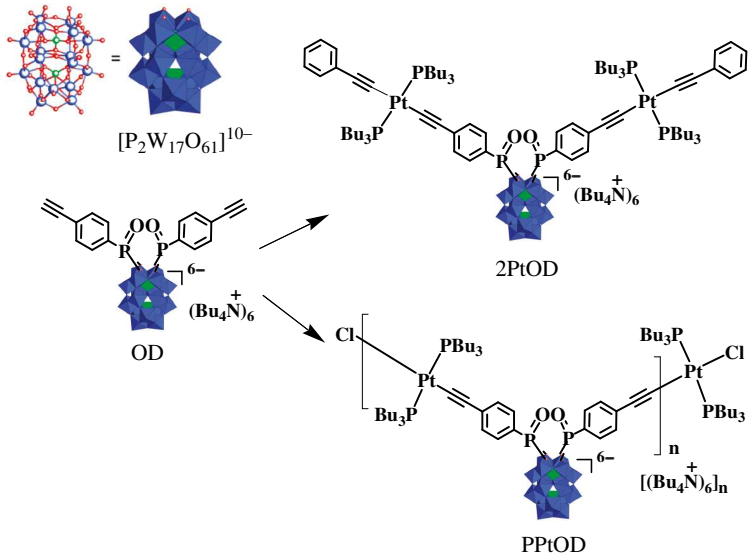

A new synthetic route for preparing Dawson-type polyoxometalate (POM) based inorganic-organic hybrid compounds (2PtOD and PPtOD) with a rigid covalent linkage between the POM and the Pt(II)-acetylide moiety is described. The redox potential of the POM polyanion can be tuned by grafting the organic and organometallic groups on it. The photoelectric properties of these hybrid LB films were studied.